Demonstrating optical-path compensation in a Michelson interferometer

N. C. Bruce and I. Montes-González

Instituto de Ciencias Aplicadas y Tecnología, Universidad Nacional Autónoma de México, Ciudad Universitaria, Ciudad de México 04510, México.

Received 25 May 2023; accepted 22 June 2023

In this paper we present a simple experiment using a fully compensated Michelson interferometer and a white-light source to demonstrate the importance and the effects of the optical-path compensation. Polyester sheets are introduced in one of the arms of the interferometer to partially decompensate the system. The change in mirror position required to see the fringes in these two cases is related to the refractive index and the thickness of the polyester sheets, and the degradation in the contrast of the white-light fringes due to the partial compensation can easily be demonstrated.

Keywords: Michelson interferometer; white-light source.

DOI: https://doi.org/10.31349/RevMexFisE.21.010204

1. Introduction

One of the basic optics undergraduate experiments is the Michelson interferometer [1-8]. Different aspects of optics can be studied with this apparatus, including interference and temporal coherence and its relationship with the spectrum of the light source, as well as displacements and the refractive index of materials [1-8]. Usually, three different types of light sources are used with the Michelson: a laser, to measure the wavelength of the light, the refractive index of air by counting fringes or displacements of one of the interferometer mirrors [3]; a gas emission lamp, commonly sodium to measure the separation between the two lines of the sodium d-line doublet [7]; and a white light source as an example of a low-coherence source to demonstrate the production of a few colored fringes in very narrow region of the mirror positions due to this low coherence [8].

To be able to obtain fringes with white light, the interferometer must be compensated by including a glass block the same size as the beamsplitter, and at the same inclination angle, to equalize the optical paths in the two arms of the device. The compensation is a question which is sometimes difficult for students to grasp, particularly when the interferometer cannot be changed to change the compensation conditions and to see the effect on the fringes.

In this paper we present a simple experiment to demonstrate the principle of compensation in a Michelson interferometer with a white-light source, which only requires a few sections of polyester sheets (we used blank slides for old overhead projectors) or microscope slides as additional material, making it a very accessible method for undergraduate teaching laboratories.

In Sec. 2 of this paper we present the theory of compensation in a Michelson interferometer, in section 3 we present the experimental results obtained and conclusions are presented in Sec. 4.

2. Theory

2.1. Compensated Michelson interferometer

Figure 1 shows the basic experimental setup for a compensated Michelson interferometer and the path of a single ray passing through the device, including the division into two parts at the first surface of the beam splitter [1]. The diffuser in front of the light source is to ensure that the light enters the interferometer with many different propagation angles to ensure a clear interference pattern. In Fig. 1, the ray which is reflected from the first surface of the beam splitter (shown in black) passes through the compensator plate, which is a glass plate made of the same material as the beam splitter, and at the same inclination angle. This ray then goes to the mirror M_1 and is transmitted back through the compensator plate and on to the beam splitter again. This ray will be split by the first surface of the beam splitter and part of it will pass through the glass of this component to be finally transmitted to the lens and detector (which can be a human eye). The ray

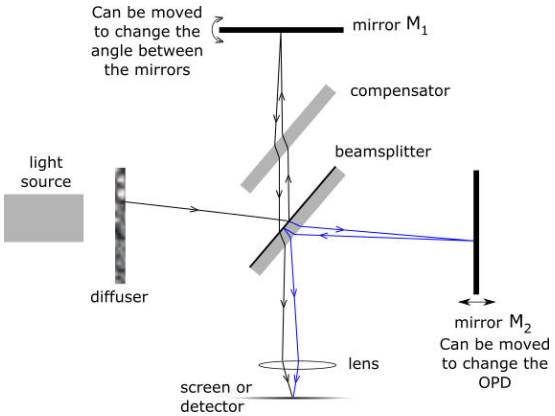

FIGURE 1. Setup for the Michelson interferometer. The path of one ray is shown, the ray is shown as black after the first reflection at the first surface of the beam splitter, and blue after the first transmission at the beam splitter, only for clarity in the figure.

which is transmitted through the first surface of the beam splitter (shown in blue) passes through the glass of this component, is reflected by mirror M_2, and comes back to the beamsplitter plate. Here, remembering that the reflecting surface of the beam splitter is the surface to the top-left of the plate, the returning ray passes through the glass of the beam splitter, is reflected and passes through the glass again. The ray finally goes to the lens and detector, to be combined with the first ray. It is important to remember that rays originating at different points on the diffuser have different, random, phases and give incoherent addition, and rays leaving the same point on the diffuser at different angles will reach different points on the detector plane, so the only interference contribution comes from the contributions of the rays described here.

In equations, the optical paths for the rays in this compensated interferometer are given by:

$$d_1 = \Delta_1 + 3n\delta\,, \tag{1}$$

$$d_2 = \Delta_2 + 3n\delta\,, \tag{2}$$

where d_i is the optical path for the ray reflected from mirror M_i, Δ_i is the distance travelled in air for the ray going from the beamsplitter to mirror M_i and back to the beamsplitter, n is the refractive index of the glass of the beamsplitter plate and the compensator plate, and δ is the distance travelled inside the glass for each pass through the beamsplitter plate. It is assumed that all the rays shown travel through the glass at approximately the same angle. Each ray in the compensated interferometer passes through a glass plate three times and this is considered in Eqs. (1) and (2). There can also be a difference in the optical paths between the two rays in the air between the beamsplitter and the detector plane, but we will assume that this term is also included in the Δ_i terms in Eqs. (1) and (2).

Now, the interference depends on the difference in optical paths of these two rays, Δd:

$$\Delta d = \Delta_2 - \Delta_1 + 3n\delta - 3n\delta = \Delta_2 - \Delta_1, \tag{3}$$

which means that the phase difference between the two rays is:

$$\Delta\phi = \frac{2\pi}{\lambda}(\Delta_2 - \Delta_1), \tag{4}$$

where Eq. (4) shows that for every wavelength λ, if $\Delta_2 - \Delta_1 = 0$, then the phase difference is 0, and all the zero-order interference fringes for all the wavelengths in the source spectrum coincide in position on the screen. This can be arranged by changing the position of mirror M_2 in Fig. 1, to change Δ_2, to cancel the value of Δ_1.This means that all the low-order fringes coincide for different wavelengths and can be seen on the screen or detector (see Fig. 2). As the order of the fringes increases the term $\Delta_2 - \Delta_1$ is no longer 0, and the phase difference, Eq. (4), depends on the wavelength λ, so the fringes for different colors have a different separation, and start to mix, giving fringes where the different colors can be seen.

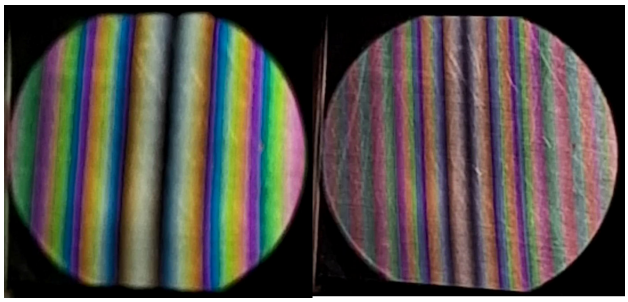

FIGURE 2. The white-light fringe pattern obtained in a compensated Michelson interferometer. (Left) image showing the center of the fringe pattern, with high contrast fringes in the center and colors appearing as the fringes for different wavelengths have different separations (note that the pattern is not exactly symmetric due to an additional phase difference between internal and external reflection in the beam splitter); (Right) the whole fringe pattern showing how the contrast is lost after a few fringes.

Finally, there is so much mixing of the fringes that only the original color of the source can be seen, Fig. 2.

2.2. Uncompensated Michelson interferometer

Now, what happens if there is no compensator in the interferometer? In this case the ray reflected on mirror M_1 will only pass through the glass plate of the beam splitter once giving:

$$d_1 = \Delta_1 + 1n\delta, \tag{5}$$

$$d_2 = \Delta_2 + 3n\delta, \tag{6}$$

and the phase difference between the two rays will be:

$$\Delta\phi = \frac{2\pi}{\lambda}\Delta d = \frac{2\pi}{\lambda}(\Delta_2 - \Delta_1 + 2n\delta). \tag{7}$$

This phase difference can only be made equal to zero when:

$$\Delta_2 - \Delta_1 = -2n\delta, \tag{8}$$

but, since the refractive index, n, changes for different wavelengths, Eq. (8) can only be satisfied for one wavelength at a time. This means that the zero-phase difference position can only be found for one wavelength at a time by changing the

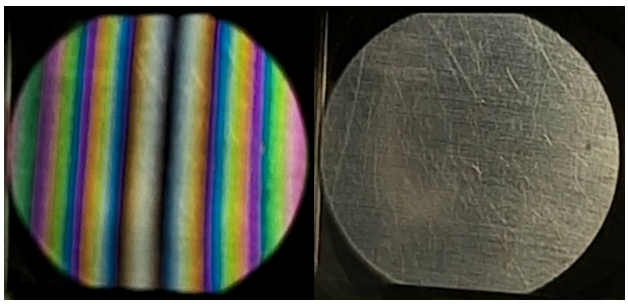

FIGURE 3. (Left) The white-light fringe pattern obtained in a compensated Michelson interferometer; (Right) The white-light uniform intensity obtained in a non-compensated Michelson interferometer.

position of mirror M_2 in Fig. 1, and therefore the zero-order positions of the different wavelengths in the spectrum of the source do not coincide. This, in turn means that the fringes for different colors are displaced from one another, as can be seen in the right side of Fig. 3, and the colors are always mixed up to give a uniform intensity the same color as the source and no visible fringes for a white-light source and a non-compensated interferometer.

2.3. Partially uncompensated Michelson interferometer

Assuming a compensated interferometer and a white-light source, with visible fringes centered on the screen or detector, the interferometer can be uncompensated by adding a piece of glass or transparent plastic in one of its arms (see Fig. 4). We assume that the extra glass or plastic is in the M_2 arm of the interferometer, but the case of having the extra glass in the other arm can easily be used with a very similar analysis. We have used a polyester sheet (a blank transparency for old overhead projectors) with a thickness of approximately 0.12 mm and a refractive index of about 1.66 [10], of which various layers are required to remove the compensation, or a microscope slide, with a thickness of approximately 1 mm and a refractive index of around 1.5, which we have found is thick enough to partially decompensate the interferometer without destroying the compensation completely, and as will be described in the results section below.

There are reflections from each surface of the additional microscope slide or polyester sheet, but they are much less intense than the reflection from interferometer mirror M_2, and we have found it impossible to detect the fringes from these extra reflections by eye, so the reflection from M_2 can be clearly seen, with a double pass through the additional glass or plastic layer.

In equations, for an originally compensated interferometer and an extra thickness of d_e in the M_2 arm:

$$d_1 = \Delta_1 + 3n\delta, \tag{9}$$

$$d_2 = \Delta_2 + 3n\delta + 2(n_e - 1)d_e, \tag{10}$$

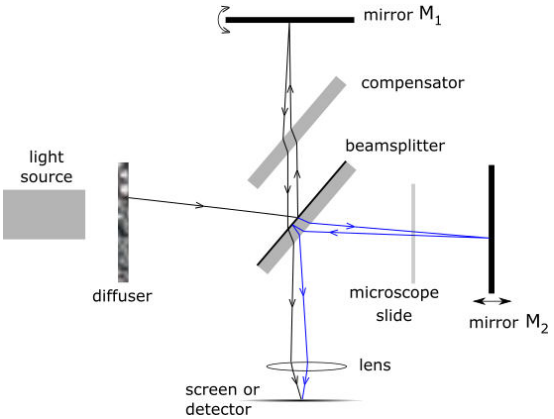

FIGURE 4. Setup for the Michelson interferometer with an additional microscope slide introduced to partially decompensate the system.

where the subscript e indicates the values for the extra material placed in the interferometer arm, for the refractive index and thickness. The term $2(n_e - 1)d_e$ is the change in the optical path when the microscope slide or polyester sheet is introduced into the interferometer, with the thickness of the slide in air being removed and replaced by glass or plastic, and the light passing through the slide twice. In this case the phase difference is now given by:

$$\Delta\phi = \frac{2\pi}{\lambda}(\Delta_2 - \Delta_1 + 2(n_e - 1)d_e). \tag{11}$$

This means that the position of mirror M_2 must be changed between the case of the compensated interferometer (without the microscope slide or polyester sheet and with the fringes centered on the screen or the detector), and the case of the partially compensated interferometer (with the microscope slide or polyester sheet and with the fringes centered on the screen or the detector). Changing the position of M_2 by a distance x changes the total optical path in that arm by $2x$, since the light has a double pass up to the mirror and back towards the beamsplitter. Then, to compensate the additional optical path, M_2 must be moved by a distance:

$$x = (n_e - 1)d_e. \tag{12}$$

It is important to note that the interferometer is no longer compensated because the refractive index of the polyester sheet or the microscope slide also depends on the wavelength, so there will be a degradation in the contrast of the fringes, but because the added samples are thin, the compensation will not be completely removed.

The distance moved by M_2, x, is proportional to the optical path change when the microscope slide or polyester sheet is introduced, meaning that this experiment can also be used to extract information on either the thickness or refractive index of the slide using Eq. (12), the other parameter (the thickness to measure the refractive index, or the refractive index to measure the thickness) must be known or estimated [9].

3. Results

As mentioned above, polyester sheets can be used to decompensate the interferometer, but in this case, as the sheets are thin, about 120 μm in width, more than one sheet is required to remove the compensation completely. The effect on the fringe contrast can be seen gradually as more sheets are added, as shown in Fig. 5. Table I shows the results of the mirror movement required to find the fringes with the polyester sheets present, and the calculated refractive index using Eq. (12) and a measured value of the slide thickness of $d_m s = 0.120 \pm 0.005$ mm. All the movements of the mirror M_2 were measured using the micrometer attached to the interferometer. For 9 polyester sheets the fringes were no longer visible and the interferometer was completely uncompensated, as shown in Fig. 3. In this case the position of

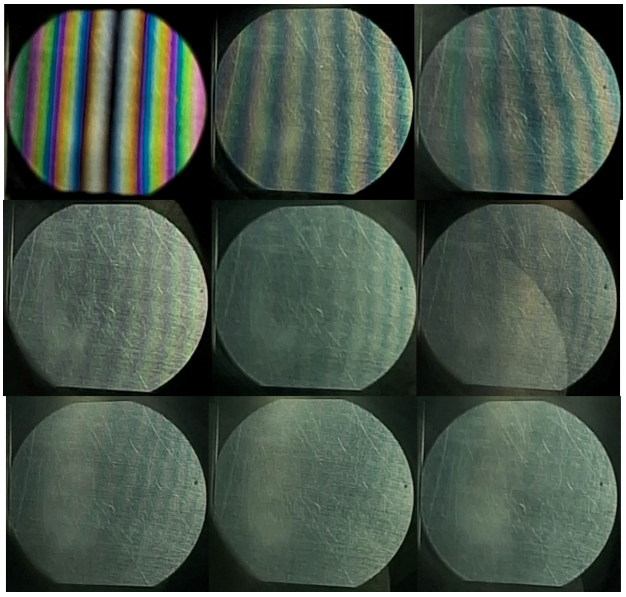

FIGURE 5. The white-light fringes for different numbers of polyester sheets, from 0 to 8, in the interferometer.

TABLE I. Mirror movement required to find the white-light fringes in the interferometer for each case, and the calculated refractive index.

Number of sheets	movement (mm)	n
1	0.086 ± 0.003	1.72 ± 0.02
2	0.170 ± 0.003	1.70 ± 0.02
3	0.256 ± 0.003	1.72 ± 0.02
4	0.340 ± 0.003	1.70 ± 0.02
5	0.424 ± 0.003	1.70 ± 0.02
6	0.508 ± 0.003	1.70 ± 0.02
7	0.592 ± 0.003	1.70 ± 0.02
8	0.676 ± 0.003	1.70 ± 0.02
9	0.760 ± 0.003	1.70 ± 0.02

mirror M_2 was determined from the average step required between the fringe positions for the cases of 1 to 8 polyester sheets, since the fringes were no longer visible.

From only a visual inspection of the fringe patterns for the different cases it is clear that the contrast of the fringes decreases as more of the additional components are added to the interferometer, but this can also be studied quantitatively by using an image analysis program such as ImageJ [11, 12], which is a free, widely used program, and which is easily accessible for students. An intensity profile can be obtained for each image, as shown in Fig. 6.

The contrast can be found using the difference in gray levels in the photographs of the fringe patterns measured by ImageJ using the equation:

$$C = \frac{I_{\max} - I_{\min}}{I_{\max} - I_{\min}}, \tag{13}$$

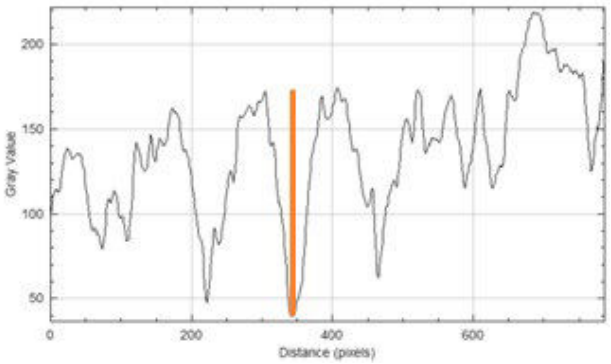

FIGURE 6. The contrast measured is given by the maximum contrast (maximum intensity to minimum intensity as shown by the orange line) in the plot profile for each case.

TABLE II. Maximum fringe contrast in the interference pattern for each case.

Number of sheets	Contrast C
No polyester sheet	0.96
1	0.26
2	0.22
3	0.16
4	0.12
5	0.13
6	0.08
7	0.1
8	0
9	0

where $I_{\max}$ and $I_{\min}$ are the maximum and minimum gray levels in the images analyzed in ImageJ. Since the fringe contrast varies over the interference pattern, the maximum contrast in each pattern, obtained near the centre of the fringe pattern, is chosen as a good parameter of comparison. The results of the contrast measurements are shown in Table II.

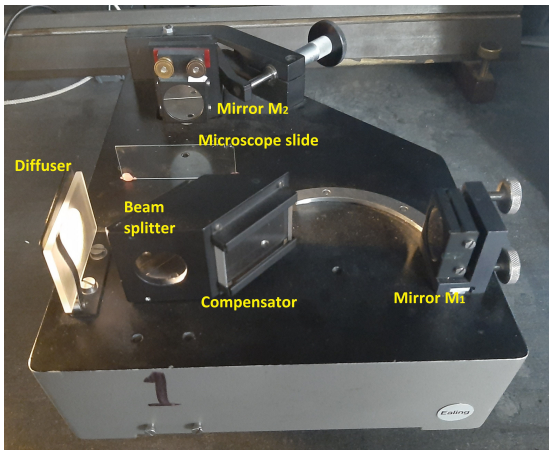

FIGURE 7. Photograph of the experimental set up including the microscope slide in one of the arms of the interferometer.

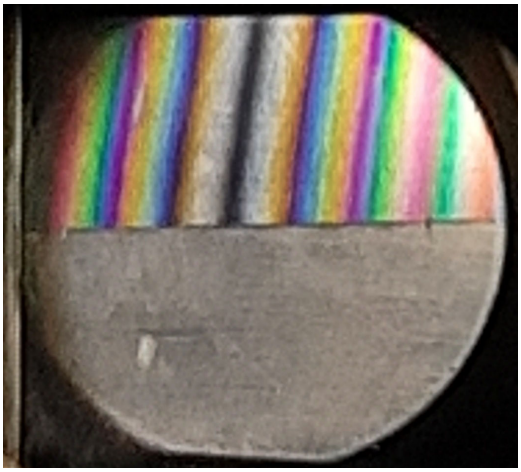

FIGURE 8. The view of the white-light fringes after introducing the microscope slide in the bottom part of the field of view before moving mirror M_2. The fringes can still be seen in the top half of the image, which is still fully compensated, but in the bottom half the fringes are no longer visible with these mirror positions.

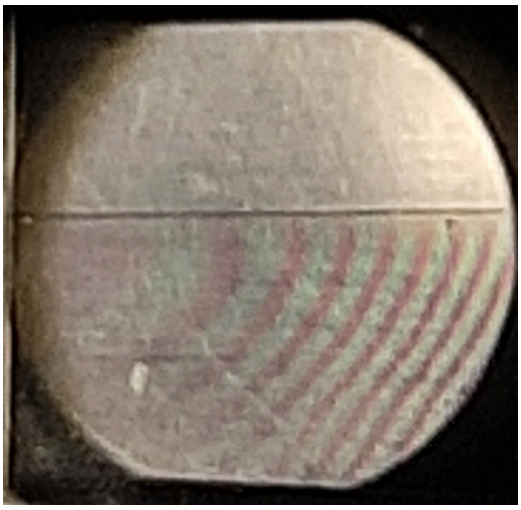

FIGURE 9. The view of the white-light fringes after moving the position of M_2 towards the beamsplitter by a distance given by Eq. (12). Fringes are now visible in the bottom half of the field of view, where the microscope slide was added.

For the cases with lower fringe contrast, the noise in the image makes it difficult to find a very precise contrast value, but the overall behaviour of a reduction of the contrast of the fringes as more material is added, is clear from Table II.

In the case of the microscope slide, it was found that adding two slides removes the compensation completely and the fringes cannot be seen. For one microscope slide, the experimental setup is as shown in Eq. (7), with the slide mounted in one arm of the interferometer such that it covered only the bottom half of the field of view, giving the fringe pattern shown in Fig. 8, with the white-light fringes visible only in the top half of the field of view. Then the mirror M_2 was moved towards the beam splitter to compensate the extra optical path introduced by replacing air in this arm of the interferometer with the glass of the microscope slide. As mirror M_2 is moved the fringes at the top of Fig. 8 move away from the field of view, meaning no fringes can be seen, and when the mirror has moved the distance given by Eq. (12) fringes will move into the bottom part of the field of view, as shown in Fig. 9. The measured value of the slide thickness was $d_m s = 0.928 \pm 0.005$ mm. The calculated refractive index using Eq. (12) and a movement of mirror M_2 of 0.4748 ± 0.0004 mm, was 1.512 ± 0.001, which is consistent with the expected value of glass. It can also be seen that the fringe shape changes in the bottom half of Fig. 9. This is due to deformations of the microscope slide and the inclination of its position in the interferometer, which can change the wavefront from this arm of the Michelson.

4. Conclusions

In this paper a simple method of demonstrating the effect of the compensation in a Michelson interferometer has been presented. This idea is sometimes difficult for students to understand, since the compensation cannot be undone to observe the effect on the fringes in the interferometer. The method proposed here uses a compensated Michelson interferometer, which is a typical undergraduate optics laboratory experiment, with a white light source, and uses polyester sheets or microscope slides to decompensate the interferometer. The position of one of the mirrors must be changed to see fringes as the additional material is added to one of the interferometer arms, and the contrast of the fringes is reduced because of the reduced compensation. The fringe contrast can be seen directly or can be measured by using an image analysis software.

Control of the interferometer compensation is important in Optical Coherence Tomography, which is used to image the eye or skin structure, as it gives a limit on the depth which can be imaged with this technique [13-17], and in other interferometric techniques which use a wide spectrum, such as absorption spectrometry, or Fourier transform spectroscopy for measuring spectra [18].

Acknowledgements

The authors thank the staff of the undergraduate optics teaching laboratory at the Facultad de Ciencias, UNAM. IvÃ¡n Montes thanks CONACyT, Mexico for a doctoral grant, DGAPA-UNAM for a grant through project IG100121, and Esperanza, formacion y vida A.C. for financial support.

1. E. Hecht and A. Zajac, Optics, (Addison-Wesley, Reading, Massachusetts, U.S.A, 1974), chapter 9
2. E.F. Cave and L.V. Holroyd, Inexpensive Michelson interferometer, *American Journal of Physics*, **23** (1955) 61, https://doi.org/10.1119/1.1933884.
3. K.G. Libbrecht and E.D. Black, A basic Michelson laser interferometer for the undergraduate teaching laboratory demonstrating picometer sensitivity, *American Journal of Physics*, **83** (2015) 409, https://doi.org/10.1119/1.4901972.
4. J.B. Diamond, D.P. Donnelly, J.D. Breault and M. McCarthy, Measuring small vibrations with interferometry, *American Journal of Physics*, **58** (1990) 9199, https://doi.org/10.1119/1.16301.
5. S.H. Yim and D. Cho, Two-frequency interferometer for a displacement measurement, *American Journal of Physics*, **81** (2013) 153, https://doi.org/10.1119/1.4746815
6. M. Vollmer and K.-P. Möllmann, Michelson interferometer for your kitchen table, *The Physics Teacher*, **46** (2008) 114 https://doi.org/10.1119/1.28345356
7. M. D'Anna and T. Corridoni, Measuring the separation of the sodium D-doublet with a Michelson interferometer, *European Journal of Physics*, **39** (2018) 015704 https://doi.org/10.1088/1361-6404/aa8e76
8. T. Fuji, M. Arakawa, T. Hattori and H. Nakatsuka, A white-light Michelson interferometer in the visible and near infrared regions, *Review of Scientific Instruments*, **69** (1998) 2854 https://doi.org/10.1063/1.1149024
9. R.M. Whittle and J. Yarwood, Experimental Physics for Students, (John Wiley and Sons Inc., New York, 1973), section 2.5(c) https://openlibrary.org/books/OL5084313M/Experimental_physics_for_students
10. I. Savukov and D. Budker, Wave-plate retarders based on overhead transparencies, *Appl. Opt*. **46** (2007) 5129, https://doi.org/10.1364/AO.46.005129
11. https://imagej.net accessed the 24th of April 2023
12. C. A. Schneider, W. S. Rasband, and K. W. Eliceiri, NIH Image to ImageJ: 25 years of image analysis. *Nature Methods*, **9** (2012) 671, https://doi:10.1038/nmeth.2089
13. K. Pepper *et al*., Full-field optical coherence tomography- An educational setup for an undergraduate lab, *American Journal of Physics*, **88** (2020) 1132. https://doi.org/10.1119/10.0001755
14. D. Huang *et al*., Optical Coherence Tomography, *Science*, **254** (1991) 1178 https://doi.org/10.1126/science.1957169
15. D. Stifter , Beyond biomedicine: A review of alternative applications and developments for optical coherence tomography, *Applied Physics B*, **88** (2007) 337 https://doi.org/10.1007/s00340-007-2743-2
16. C.A. Puliafito *et al*., Imaging of macular diseases with optical coherence tomography, *Opthalmology*, **102** (1995) 217 https://doi.org/10.1016/s0161-6420(95)31032-9
17. P.H. Tomlins, and R.K. Wang, Theory, developments and applications of optical coherence tomography, *Journal of Physics D: Applied Physics*, **38** (2005) 2519, https://doi.org/10.1088/0022-3727/38/15/002
18. J.B. Bates, Fourier transform spectroscopy, Computers and Mathematics with Applications, **4** (1978) 73, https://doi.org/10.1016/0898-1221(78)90020-2